

Phase coexistence and magnetically tuneable polarization in cycloidal multiferroics

I. Fina,^{1,*} V. Skumryev,^{2,3} D. O'Flynn,^{4,†} G. Balakrishnan,⁴ and J. Fontcuberta^{1,‡}

¹*Institut de Ciència de Materials de Barcelona (ICMAB-CSIC), Campus UAB, Bellaterra 08193, Catalonia, Spain*

²*Institució Catalana de Recerca i Estudis Avançats (ICREA), Catalonia, Spain*

³*Departament de Física, Universitat Autònoma de Barcelona, E-08193 Bellaterra, Barcelona, Spain*

⁴*Department of Physics, University of Warwick, Coventry CV4 7AL, United Kingdom*

(Received 24 January 2013; published 6 September 2013)

In some magnetic ferroelectrics the polarization \mathbf{P} direction can be selected by a magnetic field \mathbf{H} . Here we show that in a $(Y_{1-x},\text{Sm}_x)\text{MnO}_3$ single crystal, both the direction *and* the magnitude of \mathbf{P} can be controlled solely by \mathbf{H} . We argue that this remarkable dual control arises from both the phase coexistence of *bc*-cycloidal regions within an *ab*-cycloidal matrix and the annihilation of multiferroic domain walls by *H* cycling. We show that phase coexistence occurs even within the high-temperature spin-collinear phase and argue that this could be a general property arising from the strong frustration of magnetic interactions in these oxides.

DOI: 10.1103/PhysRevB.88.100403

PACS number(s): 75.85.+t, 75.60.Ch

Magnetic ferroelectrics are receiving much attention due to the intimate coupling between the magnetic order and the ferroelectric polarization.¹ First discovered in the orthorhombic TbMnO_3 perovskite, the ferroelectric polar state can be controlled by a suitable magnetic field.² The key to understanding this response was the observation that the magnetic structure of this perovskite is cycloidal, thus implying that the spins of neighboring magnetic ions ($\mathbf{S}_i, \mathbf{S}_j$) are noncollinear and rotate across the lattice in a plane containing the propagation vector of the cycloid.³ According to the current understanding, either within the so-called spin current model of Katsura, Nagaosa, and Balatsky⁴ or the inverse Dzyaloshinskii-Moriya model of Sergienko and Dagotto,⁵ the $\mathbf{S}_i, \mathbf{S}_j$ spins produce a dipolar moment $\mathbf{p}_{ij} \approx A \mathbf{r}_{ij} \times (\mathbf{S}_i \times \mathbf{S}_j)$, where \mathbf{r}_{ij} is the unit vector connecting the two ions and *A* is a constant. In the case of the cycloidal spin arrangement, all \mathbf{p}_{ij} add in phase, thus giving rise to a net polarization \mathbf{P} . Therefore, the helicity vector ($\mathbf{C} = \sum \mathbf{S}_i \times \mathbf{S}_j$) univocally determines the direction and sign of \mathbf{P} . Cycloidal order originates from a subtle competition of magnetic interactions, and thus the cycloidal plane and subsequently the polarization \mathbf{P} can be easily modified by the application of a magnetic field, as experimentally observed.² Therefore, cycloidal antiferromagnets and, most generally, antiferromagnets with a spiral or conical spin structure can display strong magnetoelectric coupling, including a magnetic-induced flop of \mathbf{P} or an electric-field-induced switch of \mathbf{C} .⁶

Whereas in cycloidal AMnO_3 [*A* = Tb (Refs. 2 and 3), Dy (Ref. 7), $\text{Gd}_x\text{Tb}_{1-x}$ (Ref. 8), $\text{Y}_{1-x}\text{Sm}_x$ (Ref. 9), $\text{Y}_{1-x}\text{Eu}_x$ (Ref. 10), etc.] perovskites the propagation direction of the spin cycloid is found to be along the orthorhombic *b* axis (*Pbnm* setting), the cycloidal plane can be either *ab* or *bc* depending on the rare earth and/or temperature. An external magnetic field can produce a flop of the cycloidal plane from *ab*(*bc*) to *bc*(*ab*), thus implying that the helicity \mathbf{C} can be flopped by 90° and, concomitantly, the polarization flops from the *a* (*c*) to *(a)* axis [\mathbf{P}_a (\mathbf{P}_c) to \mathbf{P}_c (\mathbf{P}_a)].

In the absence of any electric-field (*E*-field) poling, the \mathbf{P}_a^\pm states are degenerate and thus *H*-induced polarization coherent flop from the \mathbf{P}_c^+ (or \mathbf{P}_c^-) state should lead to equally populated \mathbf{P}_a^\pm domains, and therefore $\mathbf{P}_a = 0$ should be obtained. Intriguingly, close inspection of early² and recent experiments

on TbMnO_3 ,¹¹ MnWO_4 (Refs. 12 and 13) single crystals, and YMnO_3 thin films¹⁴ have shown that upon magnetic field and/or temperature cycling, these systems display a “memory effect” and a polarization always pointing along the initial direction is always recovered. The results described below provide the key to rationalize these observations and suggest directions to search for new multiferroics.

$(\text{Y}_{1-x},\text{Sm}_x)\text{MnO}_3$ (*YSm*) belongs to the family of orthorhombic magnetic perovskites displaying a ferroelectric character.⁹ Magnetic, structural, and dielectric characterizations of *YSm* single crystals have allowed us to determine the phase diagram of these crystals [Fig. 1(a) for $(\text{Y}_{0.5}\text{Sm}_{0.5})\text{MnO}_3$]. At about $T_N \approx 40$ K, there is a transition from a paramagnetic state to a sinusoidally modulated collinear antiferromagnetic magnetic structure. At about $T_{cy} \approx 20$ K, a *bc*-cycloidal spin structure develops and persists down to the lowest temperature. In agreement with the models described above, at $T < T_{cy}$ ferroelectricity sets in and polarization develops along the *c* axis (\mathbf{P}_c). When a magnetic field is applied along a direction contained within the cycloidal *bc* plane and perpendicular to its propagation vector ($\mu_0\mathbf{H} \parallel c$), polarization \mathbf{P}_a emerges along the *a* axis, reflecting the flopping of the *bc* cycloid towards the *ab* plane (\mathbf{P}_c to \mathbf{P}_a) [sketches in Fig. 1(a)].

Here, we explore the magnetoelectric response of a $(\text{Y}_{0.5}\text{Sm}_{0.5})\text{MnO}_3$ single crystal. In contrast to the arguments presented above, we will first show that, at low temperature, starting from a partially poled \mathbf{P}_a^+ (or \mathbf{P}_a^-) state, after consecutive polarization flopping from $\mathbf{P}_a \rightarrow \mathbf{P}_c \rightarrow \mathbf{P}_a$ induced by a suitable magnetic field ($\mu_0\mathbf{H} \parallel c$), the polarization retains the memory of the initial state. It is remarkable that successive *H*-induced $\mathbf{P}_a \rightarrow \mathbf{P}_c \rightarrow \mathbf{P}_a$ flops allow to gradually increase the final \mathbf{P}_a polarization, thus implying that the magnitude of the polarization is also tunable by a magnetic field. Finally, it is also found that polarization memory survives even when *YSm* is heated up to temperatures $T_{cy} < T < T_N$. These results are interpreted on the basis of the existence of remanent *ab*-cycloidal regions within a *bc*-cycloidal background acting as seeds for nucleation and grown from preferentially oriented domains. Similarly, seeds of cycloidal domains remain in the collinear magnetic phase and promote the growth of polar regions upon cooling.

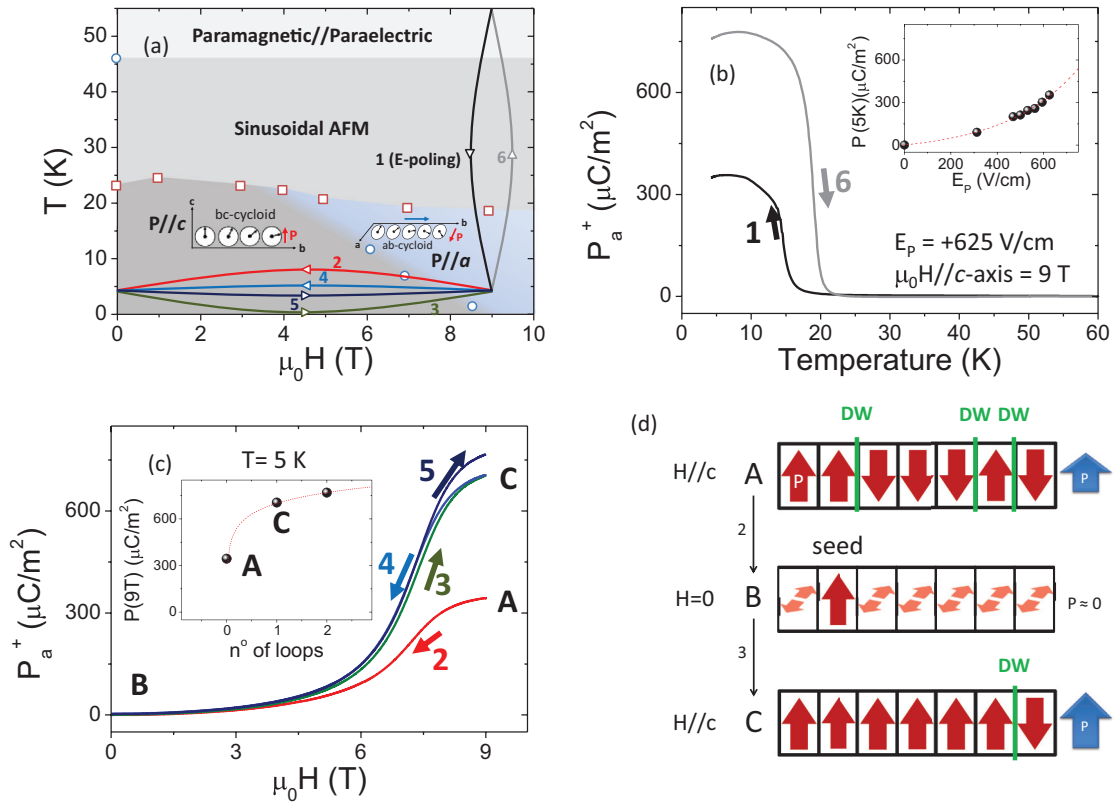


FIG. 1. (Color online) (a) Multiferroic phase diagram of YSm (adapted from Ref. 9); numbered paths indicate the thermomagnetic trajectories used in experiments. (b) Temperature dependence of the polarization after different cooling processes. Inset: Dependence of the polarization P_a^+ at 5 K on the poling field E_a . (c) Dependence of the measured polarization on magnetic field applied along the c axis. In (b) and (c) the numbers on curves indicate paths as in (a). Inset: Dependence of the polarization at 5 K, 9 T on the number of magnetic cycles (one loop corresponds to a decrease and increase in the magnetic field once). (d) Sketch of the polar domain structure after the E_a -poled cooling process and E_a zeroing, after successive H cycles. Labels in sketches A, B, and C indicate the same states as in (c). Vertical arrows represent P_a^\pm domains, and horizontal arrows represent P_c^\pm domains. Sketches do not intend to reproduce the actual population of domains. Domain walls (DW) are indicated.

$\text{Sm}_{0.5}\text{Y}_{0.5}\text{MnO}_3$ single crystals were grown by the floating zone method, and appropriately oriented and cut along the (100), (010), and (001) planes.⁹ The dimensions of the sample used here are $l_{a\text{-axis}} = 1.6(2)$ mm, $l_{b\text{-axis}} = 0.63(5)$ mm, and $l_{c\text{-axis}} = 2.45(1)$ mm. The (100) plane was contacted with silver paste¹⁵ and the electric polarization was determined from measurements of the pyrocurrent¹⁶ using an electrometer (617 Keithley). Dielectric permittivity (ϵ) was determined from measurements of the sample impedance at 10 kHz using an Agilent 4294A impedance meter. The ac magnetic measurements ($\mu_0 h_{ac} = 1$ mT; 333 Hz) under a bias $\mu_0 H$ field ($h_{ac} \parallel H$), and temperature-dependent experiments were carried out using a physical property measurement system (PPMS) from Quantum Design.

In Fig. 1(b), we show the polarization P_a measured upon cooling the sample from $T = 60$ K ($>T_N$) to 4.2 K under $\mu_0 \mathbf{H} \parallel c$ (9 T) while a poling electric field ($\mathbf{E}_a^+ = +625$ V/cm) is applied [path 1 in Fig. 1(a)]. As expected, P_a^+ emerges in the cycloidal state at ≈ 15 K, thus signaling the existence of ab cycloids; below 10 K the temperature variation of P_a^+ flattens and $P_a^+(5\text{ K}) \approx 350 \mu\text{C}/\text{m}^2$. The dependence of P on the poling electric field [see the inset of Fig. 1(b) (Ref. 17)] indicates that the polarization is not saturated, thus implying the intentionally prepared coexistence of domains

with different polarization orientations. Subsequently, the magnetic field is zeroed isothermally (5 K) and the polarization is measured [path 2 in Fig. 1(a)]. Data plotted in Fig. 1(c) (curve 2-AB) show that P_a^+ reduces gradually to zero (point B) because, in the absence of H , the ab cycloids flop back to the bc plane and correspondingly the polarization flops from P_a to P_c .

The most dramatic result is seen after successively H -increasing. As shown by the data in curve 3-BC in Fig. 1(c), and in the absence of any E poling, increasing H leads to the appearance of a robust polarization P_a^+ that, at 9 T, largely exceeds [$P_a^+ \approx 700 \mu\text{C}/\text{m}^2$ (point C)] the initial value [$\approx 350 \mu\text{C}/\text{m}^2$ (point A)] which was obtained by cooling under $\mathbf{E}_a^+ = +625$ V/cm. Repeating the process of H zeroing, curve 4-CB [Fig. 1(c)] leads to P_a^+ reduction, and a subsequent H increase again leads to a further enhancement of polarization ($P_a^+ \approx 750 \mu\text{C}/\text{m}^2$) [curve 5, Fig. 1(c)]. Finally, while increasing the temperature again, the polarization gradually reduces and vanishes at around 20 K [curve 6, Fig. 1(b)]. Therefore successive H -induced flopping of the helicity of the cycloidal order leads to a progressive enhancement of polarization, as summarized in the inset of Fig. 1(c). A similar behavior is obtained after positive or negative E -field poling,¹⁸ thus excluding that ferroelectric imprint is responsible for the measured effect. Therefore, data in Fig. 1(c) show that

(a) H cycling produces flopping of bc to ab cycloids and the concomitant variation of \mathbf{P}_a^+ , however, (b) the orientation of \mathbf{P}_a^+ domains is not erased and \mathbf{P}_a^+ domains reappear after successive $\mu_0\mathbf{H} \parallel c$ -induced flops, and (c) \mathbf{P}_a^+ reinforces upon successive polarization flops.

To account for these observations, probably the simplest scenario is to consider that upon cooling the sample from $T > T_N > T_{cy}$, under $\mu_0\mathbf{H} \parallel c$ bias and \mathbf{E}_a^+ poling, ab -cycloidal domains are formed but either bc domains are still present or the poling field is not strong enough to produce a single \mathbf{P}_a domain state. Indeed, as indicated by the data in Fig. 1(c), the polarization \mathbf{P}_a^+ observed after step (1) is smaller than its saturation value, thus implying the coexistence of polar domains with different polarization directions, as illustrated by sketch A in Fig. 1(d). By zeroing H , most \mathbf{P}_a^+ domains are reverted to \mathbf{P}_c^+ due to the ab - to bc -cycloid flop, but some residual \mathbf{P}_a^+ domains remain [indicated as the seed domain in B in Fig. 1(d)]. By the same token, when increasing H again, these residual \mathbf{P}_a^+ domains, retaining the memory of the initial polarization state, act as seeds favoring polarization along \mathbf{P}_a^+ [Fig. 1(c), curve 3]. Cycling H again leads to an increase of the polarization along the initial direction. The key to explaining the observed memory effect and polarization enhancement

upon H cycling is the coexistence of ab - and bc -cycloidal domains deep in the cycloidal region (in which the magnetic ordering of Sm can play some role), and the suppression of the multiferroic domain walls upon H cycling [Fig. 1(d)]. The \mathbf{P}_a^+ increasing upon successive magnetic cycling also indicates that the magnetic field is more effective in orienting cycloidal domains than the E field. This is consistent with the relatively smaller electrostatic energy ($\approx EP$) available to switch the helicity vector compared to the magnetic anisotropy and the Zeeman energy.¹⁹

Having established the coexistence of different cycloidal domains at $T < T_{cy}$, we address now the possible existence of cycloidal domains in the temperature region ($T_{cy} < T < T_N$) where an average collinear spin order exists. This issue is addressed by performing the following experiments. First the sample is cooled from $T \gg T_N$ to the lowest temperature (5 K) under $\mu_0\mathbf{H} \parallel c$ (9 T) and $\mathbf{E}_a^+ = +625$ V/cm. Next, the \mathbf{E}_a^+ bias field is zeroed ($\mathbf{E}_a^+ = 0$) and the sample is heated up to a temperature T_R and again cooled down to 5 K. The polarization $\mathbf{P}_a^+(T, T_R)$ is subsequently measured while heating [Fig. 2(a)]. Data in this figure show that the largest polarization (≈ 350 $\mu\text{C}/\text{m}^2$ at 5K) is obtained when the sample is cooled down from $T_R \leq 17.5$ K (i.e., $T_R < T_{cy}$), as expected for an

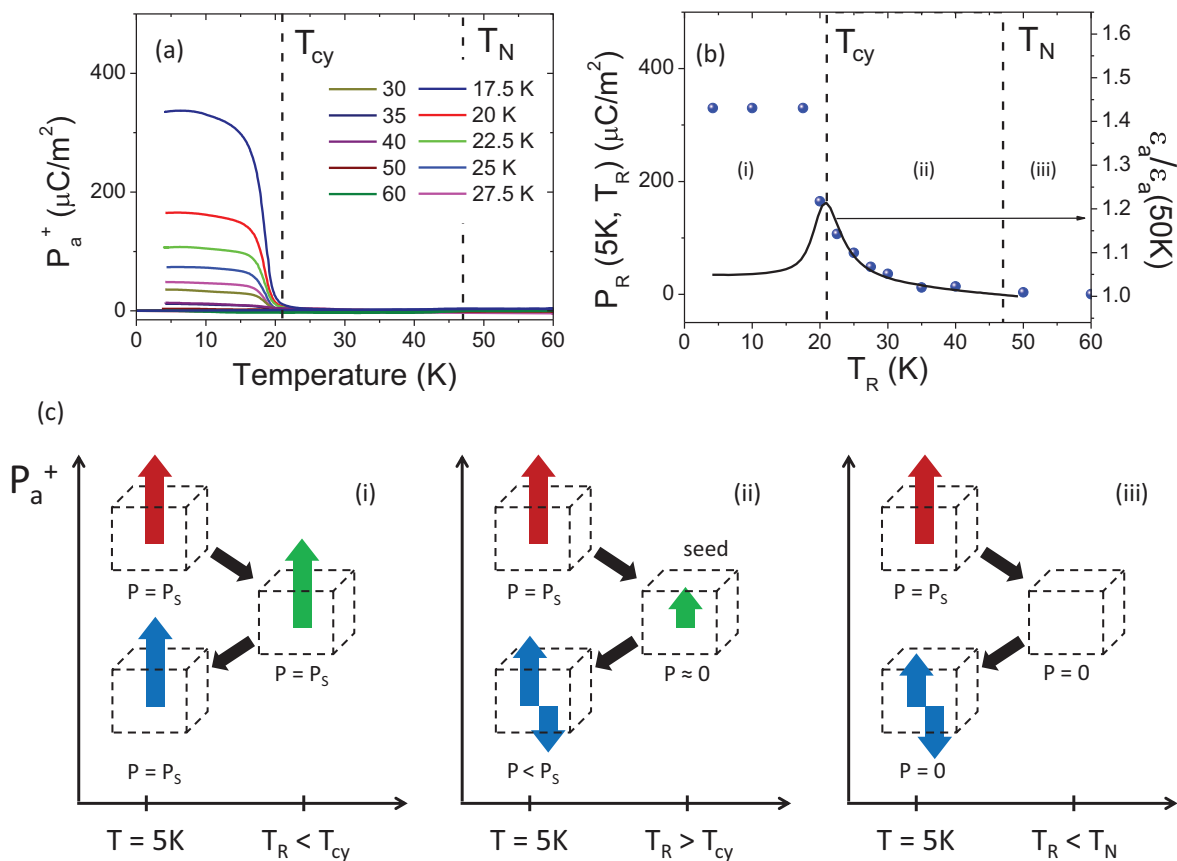


FIG. 2. (Color online) (a) Polarization vs temperature (measured upon heating from 5 K) as a function of the temperature T_R at which the sample has been heated prior to measurement, without any E poling. The initial low-temperature state is defined by cooling the samples under $\mathbf{E}_a^+ = 625$ V/cm and $\mu_0\mathbf{H} \parallel c$. See the text for experimental details. (b) Left axis: Dependence of the polarization at 5 K on T_R (solid symbols). Right axis: The solid line is the dielectric permittivity recorded upon heating. (c) Sketch of the initial (5 K) polarization state of the sample (red arrows) after heating to T_R (green arrows) and after subsequent cooling to 5 K without any E bias (blue arrows). Saturation polarization (P_s) corresponds to the measured polarization after E -field poling. Panels (i), (ii), and (iii) correspond to the same temperature regions as in (b).

\mathbf{E}_a^+ -poled sample containing mostly ab domains. Figure 2(b) summarizes the low-temperature $\mathbf{P}_a^+(5\text{ K}, T_R)$ values (solid symbols). Data in Fig. 2(b) show three well defined regions: (i) At $T_R < T_{cy}$, $\mathbf{P}_a^+(5\text{ K}, T_R)$ is insensitive to the precise value of T_R , thus indicating that heating and cooling the sample within the cycloidal region does not produce any modification of polarization and (iii) when $T_R > T_N$, the polarization vanishes, i.e., $\mathbf{P}_a^+(5\text{ K}, T_R) \approx 0$, indicating that without any E bias, similar amounts of ab domains with helicities \mathbf{C}_c^\pm are formed upon cooling from T_R . More interesting, in region (ii) a finite $\mathbf{P}_a^+(5\text{ K}, T_R)$ is measured, indicating that even if the sample is heated up to a temperature well into the collinear spin region ($T_N > T_R > T_{cy}$), upon subsequent cooling, a polarization along the initial poling direction is recovered. This implies that in the spin-collinear/paraelectric regime, some self-poling exists that drives the nucleation of \mathbf{P}_a^+ domains upon cooling. Most likely, polarized ab -cycloidal domains, surviving within the collinear phase, act as seeds for domain growth and hold the key to the observed polarization memory effect. Data recorded after successive temperature cycles are fully consistent with the description given above.²⁰

The presence of these polar regions within the spin-collinear region should lead to an enhanced permittivity, mimicking relaxor-like behavior. Figure 2(b) shows (solid line) the measured permittivity as a function of temperature $\varepsilon(T)$. Indeed, a noticeable enhancement of permittivity is observed upon lowering the temperature below T_N , reflecting the increasing abundance and/or size of these polar/noncollinear spin regions upon cooling below T_N but still within the collinear spin region. Moreover, it can be appreciated that in region (ii) ($T_{cy} < T < T_N$), $\varepsilon(T)$ closely follows $P_R(T)$, thus clearly supporting the view that these mesoscopic regions act as seeds for polarization growth upon further cooling.

Figure 3 (inset) shows the temperature-dependent magnetic ac susceptibility χ ($H = 0$); the Néel ($T_N \approx 47\text{ K}$) and the $T_{cy} \approx 24\text{ K}$ transitions can be clearly identified. The magnetic-field dependence $\chi(H)$ recorded at 8 K with $H \parallel c$ is also shown in Fig. 3. Solid symbols (squares and circles) correspond to data collected by increasing or reducing H , respectively; the arrows also indicate the sense of variation of H . The maxima of $\chi(H)$ at about 6.5 T reflects the flopping of the cycloids from the bc to ab planes. Of relevance here is the observation that when retreating H there is a clear hysteresis that signals the persistence of the high- H phase (ab cycloids) within the low- H phase (bc cycloids). Triangle symbols (open) on these curves are susceptibility data measured, isothermally, at some particular values of H back from $H = 0$. Data closely follow the retreating curve, thus indicating the robust persistence of ab cycloids even after zeroing H . Only when the crystal is heated above T_N and H is increased again (open rhombuses), the initial susceptibility curve is followed. Heating at some intermediate temperature ($T_{cy} < T < T_N$) only leads to a partial suppression of the hysteresis.²¹ Therefore, magnetic data conclusively show the coexistence of ab - and bc -cycloidal domains in some regions of the phase diagram and the persistence of these domains with the collinear magnetic region.

The coexistence of residual magnetic cycloidal domains within the collinear phase could be a signature of a first-order

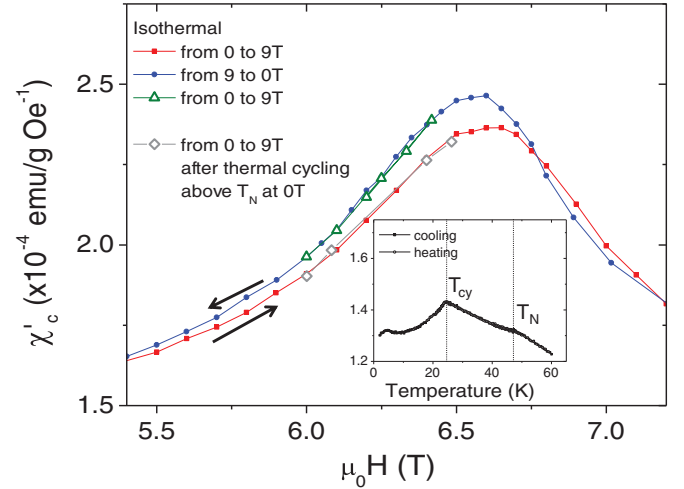


FIG. 3. (Color online) Inset: Temperature dependence of the real component of the magnetic susceptibility ($\mu_0 h_{ac} \parallel c$ axis; $H = 0$). Field dependence ($\mu_0 H$ from 0 to 9 T and to 0 T) of the real component of the magnetic susceptibility at 8 K. Solid symbols (squares and circles) correspond to data collected by increasing or reducing H , respectively; the arrows indicate the sense of variation of H . Triangle symbols (open) are susceptibility data measured, at 8 K, at some particular values of H back from $H = 0$. Open rhombuses correspond to data collected after heating the crystal to above T_N , cooled down to 8 K under zero field, and H increased again.

transition (consistent with the thermal hysteresis shown by polarization and dielectric permittivity in Ref. 22). Alternatively, either induced by local disorder in the crystal, or by short-range magnetic correlations enhanced by competing magnetic interactions, and anticipating the long-range cycloidal order, noncollinear magnetic regions could be formed, which, in presence of the inverse Dzyaloshinskii-Moriya effect, would produce confined breaking of space symmetry and thus giving rise to polar mesoregions. Notice that within this view, these polar regions result from the inherent magnetic frustration in the lattice and could lead to visible effects even within the paramagnetic phase. This is in agreement with recent observations in MnWO_4 .¹³

It is worth noticing that the absence of long-range dipolar magnetic order does not necessarily imply that the system is time-reversal invariant and magnetoelectric coupling can still be present. Indeed, it has been proposed that toroidal moments ($\tau \approx \sum \mathbf{r}_i \times \mathbf{S}_i$) in some spin-glass systems, such as $\text{Ni}_{1-x}\text{Mn}_x\text{TiO}_3$ (Ref. 23) or the trilinear spin coupling ($\chi = \mathbf{S}_i(\mathbf{S}_j \times \mathbf{S}_k)$) in some spin liquids such as $\text{YBaCo}_3\text{FeO}_7$,²⁴ may give rise to polarization and magnetoelectric coupling.

In summary, we have seen that in orthorhombic antiferromagnets, where the high-temperature paramagnetic phase ($T > T_N$) is separated from the low-temperature bc -cycloidal phase occurring at T_{cy} by a region ($T_{cy} < T < T_N$) of collinear magnetic order, the polarization, when modified by appropriate magnetic field or temperature sweeps, retains memory of its initial state and thus the polar state can be univocally determined without the need for electric poling. We argue that these effects arise from the coexistence of cycloidal domains, either ab or bc depending on the experimental conditions, within the cycloidal region ($T < T_{cy}$) or even within the

collinear ($T_{cy} < T < T_N$) region. These polar regions, acting as a poling field, determine the direction of polarization after subsequent H flops, thus providing a simple explanation for the observed memory of the polarization state, and are the key to avoiding energy-costly domain wall formation, and thus being instrumental in determining the magnitude of the observed magnetic-field-induced polarization enhancement. We argue that mesoscopic phase separation in these oxides is probably inherent and results from the strongly competing nature of the existing magnetic interactions. Either resulting from short-range magnetic correlations, martensitic-like strains generated across phase transitions, or by defect-associated local disorder, these polar regions allow the polarization of these oxides to be fully controllable exclusively by a magnetic field. It

thus follows that polar regions could be present in other non-collinear and magnetically frustrated magnetic systems, with potentially interesting dielectric properties. Our results and some recent reports, call for a deep search of the dielectric response, within the paramagnetic regime, of frustrated magnetic systems.

ACKNOWLEDGMENTS

Financial support by the Spanish Government (Projects MAT2011-29269-C03 and CSD2007-00041) and Generalitat de Catalunya (2009-SGR-00376) is acknowledged. G.B. wishes to thank EPSRC, UK for financial support through Grant EP/I007210/1.

*ignasifinamartinez@gmail.com

†Present address: Department of Medical Physics and Bioengineering, Malet Place Engineering Building, University College London, WC1E 6BT.

‡fontcuberta@icmab.cat

¹W. Eerenstein, N. D. Mathur, and J. F. Scott, *Nature (London)* **442**, 759 (2006); M. Fiebig, *J. Phys. D* **38**, R123 (2005); N. A. Spaldin and M. Fiebig, *Science* **309**, 391 (2005); C. N. R. Rao, A. Sundaresan, and Rana Saha, *J. Phys. Chem. Lett.* **3**, 2237 (2012).

²T. Kimura, T. Goto, H. Shintani, K. Ishizaka, T. Arima, and Y. Tokura, *Nature (London)* **426**, 55 (2003).

³M. Kenzelmann, A. B. Harris, S. Jonas, C. Broholm, J. Schefer, S. B. Kim, C. L. Zhang, S.-W. Cheong, O. P. Vajk, and J. W. Lynn, *Phys. Rev. Lett.* **95**, 087206 (2005).

⁴H. Katsura, N. Nagaosa, and A. V. Balatsky, *Phys. Rev. Lett.* **95**, 057205 (2005).

⁵I. A. Sergienko and E. Dagotto, *Phys. Rev. B* **73**, 094434 (2006).

⁶T. Kimura, *Annu. Rev. Condens. Matter Phys.* **3**, 93 (2012); Y. Tokura and S. Seki, *Adv. Mater.* **22**, 1554 (2010); Y. Tokura and N. Kida, *Philos. Trans. R. Soc., A* **369**, 3679 (2011); T. Arima, *J. Phys. Soc. Jpn.* **80**, 052001 (2011); K. Taniguchi, N. Abe, H. Umetsu, H. A. Katori, and T. Arima, *Phys. Rev. Lett.* **101**, 207205 (2008); H. Murakawa, Y. Onose, F. Kagawa, S. Ishiwata, Y. Kaneko, and Y. Tokura, *ibid.* **101**, 197207 (2008); N. Abe, K. Taniguchi, S. Ohtani, H. Umetsu, and T. Arima, *Phys. Rev. B* **80**, 020402(R) (2009); N. Abe, K. Taniguchi, H. Sagayama, H. Umetsu, and T. Arima, *ibid.* **83**, 060403 (2011); K. Kimura, H. Nakamura, K. Ohgushi, and T. Kimura, *ibid.* **78**, 140401(R) (2008).

⁷T. Kimura, G. Lawes, T. Goto, Y. Tokura, and A. P. Ramirez, *Phys. Rev. B* **71**, 224425 (2005); T. Goto, T. Kimura, G. Lawes, A. P. Ramirez, and Y. Tokura, *Phys. Rev. Lett.* **92**, 257201 (2004).

⁸Y. Yamasaki, H. Sagayama, N. Abe, T. Arima, K. Sasai, M. Matsuura, K. Hirota, D. Okuyama, Y. Noda, and Y. Tokura, *Phys. Rev. Lett.* **101**, 097204 (2008).

⁹D. O'Flynn, C. V. Tomy, M. R. Lees, A. Daoud-Aladine, and G. Balakrishnan, *Phys. Rev. B* **83**, 174426 (2011); D. O'Flynn, Ph.D. thesis, University of Warwick, 2010.

¹⁰S. Ishiwata, Y. Kaneko, Y. Tokunaga, Y. Taguchi, T. H. Arima, and Y. Tokura, *Phys. Rev. B* **81**, 100411(R) (2010).

¹¹D. Senff, P. Link, N. Aliouane, D. N. Argyriou, and M. Braden, *Phys. Rev. B* **77**, 174419 (2008).

¹²K. Taniguchi, N. Abe, S. Ohtani, and T. Arima, *Phys. Rev. Lett.* **102**, 147201 (2009).

¹³T. Finger, D. Senff, K. Schmalzl, W. Schmidt, L. P. Regnault, P. Becker, L. Bohatý, and M. Braden, *Phys. Rev. B* **81**, 054430 (2010).

¹⁴I. Fina, L. Fábrega, X. Martí, F. Sánchez, and J. Fontcuberta, *Phys. Rev. Lett.* **107**, 257601 (2011).

¹⁵See Supplemental Material 1 at <http://link.aps.org/supplemental/10.1103/PhysRevB.88.100403> for a detailed description of the sample preparation for dielectric measurements.

¹⁶See Supplemental Material 2 at <http://link.aps.org/supplemental/10.1103/PhysRevB.88.100403> for complementary data on dielectric permittivity and polarization dependence on temperature.

¹⁷See Supplemental Material 3 at <http://link.aps.org/supplemental/10.1103/PhysRevB.88.100403> for polarization dependence on temperature and E poling, used to extract the $P(5\text{ K})$ values.

¹⁸See Supplemental Material 4 at <http://link.aps.org/supplemental/10.1103/PhysRevB.88.100403> for polarization dependence on the magnetic field, irrespective of the E -poling sign.

¹⁹T. Hoffmann, P. Thielen, P. Becker, L. Bohatý, and M. Fiebig, *Phys. Rev. B* **84**, 184404 (2011).

²⁰See Supplemental Material 5 at <http://link.aps.org/supplemental/10.1103/PhysRevB.88.100403> for the dependence of P after successive thermal cycling.

²¹See Supplemental Material 6 at <http://link.aps.org/supplemental/10.1103/PhysRevB.88.100403> for magnetic-field dependence of the ac susceptibility for different T_R cooling temperatures.

²²See Supplemental Material 7 at <http://link.aps.org/supplemental/10.1103/PhysRevB.88.100403> for the dependence of P and dielectric permittivity on temperature for positive and negative temperature rates.

²³Y. Yamaguchi, T. Nakano, Y. Nozue, and T. Kimura, *Phys. Rev. Lett.* **108**, 057203 (2012).

²⁴D. D. Khalyavin, P. Manuel, and L. C. Chapon, *Phys. Rev. B* **85**, 220401(R) (2012).